New pyrrolo[3,2-b]pyrroles with AIE characteristics with dichloromethane and chloroform molecules detection

Shuning Yu[1], Shaoling Li[1], Zhixin Xie[1], Wei Liu[1], Md. Monarul Islam[2]*, Carl Redshaw[3], Mei Juan Cao[4]*, Qing Chen[5]*, Xing Feng[1]*

[1]Guangdong Provincial Key Laboratory of Functional Soft Condensed Matter, School of Material and Energy, Guangdong University of Technology, Guangzhou 510006, P. R. China, E-mail: hyxhn@sina.com

[2]Synthesis Laboratory, Chemical Research Division, Bangladesh Council of Scientific and Industrial Research (BCSIR) Dhanmondi, Dhaka-1205, Bangladesh. E-mail: mmipavel@yahoo.com

[3]Chemistry, School of Natural Sciences, University of Hull, Hull, Yorkshire HU6 7RX, UK.

[4]Beijing Institute of Graphic Communication, Beijing 102600, P. R. China. Email: caomeijuan@bigc.edu.cn

[5]Eco-Environmental Protection Company, China South-to -North Water Diversion Corporation Limited , Beijing 100036, China. Email: chen.qing@craes.org.cn

*Corresponding author

E-mail address: hyxhn@sina.com (X. Feng), mmipavel@yahoo.com (M. M. Islam), chen.qing@craes.org.cn (Q. Chen)

ABSTRACT

Three new pyrrolo[3,2-b]pyrroles derivatives containing methoxyphenyl, pyrene or tetraphenylethylene (TPE) units **1−3** have been designed, synthesized and fully characterized. The aggregation-induced emission (AIE) properties of compounds **1−3** were tested in different water fraction (f_w) of tetrahydrofuran (THF). The pyrrolo[3,2-b]pyrrole derivative **3** containing tetraphenylethylene units exhibited typical AIE features with an enhanced emission (~32-fold) in the solid state *versus* in solution; compounds **1** and **2** exhibited an aggregation-caused quenching effect. In addition, the steric and electronic effects of the peripheral moieties on the emission behavior, both in solution and in the solid state, have been investigated. Moreover, pyrrolo[3,2-b]pyrrole **1** exhibits high sensitivity and selectivity for dichloromethane and chloroform solvents, with the system displaying a new emission peak and fast response time under UV irradiation.

Keywords: Pyrrolo[3,2-b]pyrroles, Aggregation-induced emission (AIE), Structure-Properties relationship, Dichloromethane and chloroform molecules detection

1. INTRODUCTION

The ongoing development of new fluorescent dyes and their application as fluorescent probes containing pyrene[1−4] or tetraphenylethylene (TPE)[5−8] moieties has expanded the need for dyes with diverse spectral and physicochemical properties. Since 1,2,4,5-tetraaryl-1,4-dihydropyrrolo[3,2-b]pyrroles (TAPPs) were synthesized via a one-pot multicomponent reaction, this category of compound has attracted great attention due to their diverse selection of substituent groups, tunable electronic properties, and fantastic optical properties.[9] On the other hand, 10-π electron heterocyclic pyrrolo[3,2-b]pyrroles have been investigated for electronic devices, such as solar cells, transistors, and electrochromic devices.[10−15] Among them, 1,4-dihydro-pyrrolo[3,2-b]pyrroles are exceptionally electron-rich heteropentalenes, but the development of new pyrrolo[3,2-b]pyrroles still remains a challenge, due to the lack of an efficient synthetic methodology which can improve the final yield.[16]

Propeller-shaped molecules have attracted considerable attention since the aggregation-induced emission (AIE) phenomenon was first described.[17,18] Over the years, such skeletons, *i.e.*, hexaphenylsiloles, tetraphenylethylene (TPE) derivatives, polyphenylenes, tetraphenylthieno[3,2-b]thiophene *S*,*S*-dioxide, and diphenylbenzo[b]thiophene *S*,*S*-dioxide have been widely used in the design of new AIEgens.[19−22] Molecules exhibiting AIE character have been used as components in OLEDs and field effect transistors and as fluorescent probes. [23−25]

1,4-Dihydrotetraarylpyrrolo[3,2-b]pyrroles have been utilized in a significant number of applications, such as in the study of excited states,[26] two-photon absorptions,[27] direct solvent probing via H-bonding interactions,[28] photochromic analysis of halocarbons,[29] fluorescence probes,[30] dye-sensitized solar cells,[31] bulk heterojunction organic solar cells,[32] organic light-emitting diodes,[33] resistive memory devices,[34] aggregation induced emission,[35] and in the construction of MOFs.[36,37] Li *et al*. reported 1,4-dihydropyrrolo-[3,2-b]pyrrole-based organic dyes containing tetraphenyl ethylene (TPE), which exhibited excellent photovoltaic performance and photocatalytic activities. These attributes were mainly due to the efficient suppression of electron recombination by the special structure of the 1,4-dihydropyrrolo-[3,2-b]pyrroles unit and the tunable electron properties of the conjugated bridge.[38] The increasing interest in pyrrolo[3,2-b]pyrrole chemistry undoubtedly hinges upon better access to these heterocyclic compounds, however the problem of scalability might significantly hamper further development of their applications. Furthermore, Li *et al*. synthesized new AIEgens based on 2,5-bis(4-alkoxycarbonylphenyl)-1,4-diaryl-1,4-dihydropyrrolo[3,2-b] pyrrole in 43% yield, which served as multifunctional materials for a reversible fluorescent thermometer and a “turn-on” fluorescent probe for Cd(II) detection.[30]

Inspired by the above-mentioned results, herein we have designed and synthesized new TAPP-based organic dyes, which contains methoxyphenyl, pyrene or tetraphenylethylene units at the 1-, 2-, 4- and 5-positions of the pyrrolo[3,2-b]pyrroles. The thermal stability, optical properties, and AIE characteristics were thoroughly investigated. Moreover, compound **1** displays high sensitivity toward the solvents CH_2Cl_2 and $CHCl_3$ under UV irradiation, with a visible red-shifted emission.

2. EXPERIMENTAL SECTION

Materials

All reagents were purchased from commercial vendors and used were as received unless otherwise noted. The UV–vis and fluorescence spectroscopy was measured in spectroscopically pure reagents.

Characterization

^{1}H and ^{13}C NMR spectra were recorded on a Bruker AVANCE III 400M/600M spectrometer using chloroform-*d* solvent and tetramethylsilane as internal references; *J*-values are given in Hz. High-resolution mass spectra (HRMS) were taken on a LC/MS/MS, which consisted of an HPLC system (Ultimate 3000 RSLC, Thermo Scientific, USA) and a Q Exactive Orbitrap mass spectrometer. UV-vis absorption spectra and Photoluminescence (PL) spectra were recorded on a Shimadzu UV-2600 and a Hitachi F-4700 fluorescence spectrometer. PL quantum yields were measured using absolute methods using a Hamamatsu C11347-11 Quantaurus-QY Analyzer. The quantum chemistry calculations were performed using the Gaussian 09W (RB3LYP/6-311G(d,p) basis set) software package and BDF[39-42] of Device Studio.

2.1 Synthesis of pyrrolo[3,2-b]pyrroles derivatives 1

In a 100 mL two-necked flask, a mixture of 4-methoxybenzaldehyde (2.0 mmol, 272 mg, 1.0 eq.), 4-methoxyaniline (2.0 mmol, 246 mg, 1.0 eq.) and *p*-toluenesulphonic acid (0.2 mmol, 34.4 mg, 0.1 eq.) was added into glacial acetic acid (4 mL). The mixture was stirred at 90 °C for 30 min. After cooling to room temperature, butane-2,3-dione (1.0 mmol, 87.6 μL, 0.5 eq.) was slowly added dropwise into the reaction mixture and the system was rapidly stirred at 90 °C for 19 h. Then the mixture was cooled to room temperature and quenched with water (30 mL), and the solution was extracted three times with dichloromethane (3x 50 mL). The organic layer was washed with water (2x 20 mL) and saturated brine (50 mL), and the solution was dried by anhydrous magnesium sulfate. Filtration followed by removal of solvent afforded a residue which was purified by column chromatography using hexane and dichloromethane (V_{hexane}: $V_{CH_2Cl_2}$ =4:1) as eluent to afford compound **1** as a yellow solid in 5% yield (26.5 mg): ^{1}H NMR (400 MHz, $CDCl_3$) δ 7.21 (d, *J* = 8.9 Hz, 4H), 7.14 (d, *J* = 8.1 Hz, 4H), 6.88 (d, *J* = 8.9 Hz, 4H), 6.77 (d, *J* = 8.7 Hz, 4H), 6.26 (s, 2H), 3.83 (s, 6H), 3.78 (s, 6H) ppm. ^{13}C NMR (100 MHz, $CDCl_3$) δ 158.0, 157.4, 133.4, 129.5, 126.5, 114.3, 113.6, 93.1, 55.5, 55.2 ppm. HRMS (FTMS + p APCI): m/z+H$^+$ calcd for $C_{34}H_{30}N_2O_4$ 531.2278, found 531.2273.

2.2 Synthesis of pyrrolo[3,2-b]pyrrole derivatives 2

In a 100 ml two-necked flask, a mixture of pyrene-1-carbaldehyde (1.0 mmol, 230 mg, 1.0 eq.), 4-methoxyaniline (1.0 mmol, 123 mg, 1.0 eq.) and *p*-toluenesulphonic acid (0.1 mmol, 17.2 mg, 0.1 eq.) was added into glacial acetic acid (4 mL). The mixture was stirred at 90 °C for 30 min. After cooling to room temperature, butane-2,3-dione (0.5 mmol, 43.8 μ L, eq.) was slowly added dropwise into the reaction mixture and rapidly stirred at 90 °C for 19 h. Then the mixture was cooled to room temperature and quenched with water (30 mL), and the solution was extracted three times with dichloromethane (3x 50 mL). The organic layer was washed with water (2x 20 mL) and saturated brine (50 mL), and the solution was dried over anhydrous magnesium sulfate. Following filtration, volatiles were removed *in-vacuo*, and the resulting residue was purified by column chromatography using hexane and dichloromethane (V_{hexane}: V_{CH2Cl2} =2:1) as eluent to afford compound **2** as a green solid in 8% yield (30 mg): ^{1}H NMR (400 MHz, $CDCl_3$) δ 8.59 (d, *J* = 8.6 Hz, 2H), 8.18 (d, *J* = 7.7 Hz, 2H), 8.15 (d, *J* = 7.6 Hz, 2H), 8.12 – 7.96 (m, 10H), 7.88 (d, *J* = 7.9 Hz, 2H), 7.20 (d, *J* = 9.0 Hz, 4H), 6.67 (d, *J* = 9.2 Hz, 6H), 3.66 (s, 6H) ppm. ^{13}C NMR (100 MHz, $CDCl_3$) δ 157.0, 133.7, 133.2, 131.5, 131.1, 131.0, 130.3, 129.8, 129.2, 129.1, 127.5, 127.4, 126.0, 125.9, 125.7, 125.1, 125.0, 124.9, 124.4, 114.2, 97.0, 55.3 ppm. HRMS (FTMS + p APCI): m/z+H^+ calcd for $C_{52}H_{34}N_2O_2$ 719.2693, found 719.2682.

2.3 Synthesis of pyrrolo[3,2-b]pyrrole derivatives 3

In a 100 ml two-necked flask, a mixture of 4-(1,2,2-triphenylvinyl)benzaldehyde (1.0 mmol,360mg, 1.0 eq.), 4-methoxyaniline (1.0 mmol, 123 mg, 1.0 eq.) and *p*-toluenesulphonic acid (0.1 mmol, 17.2 mg, 0.1 eq.) was added into glacial acetic acid (4 mL). The mixture was stirred at 90 °C for 30 min. After cooling to room temperature, butane-2,3-dione (0.5 mmol, 43.8μL, 0.5 eq.) was slowly added dropwise into the reaction mixture and the system was rapidly stirred at 90 °C for 19 h. Then the mixture was cooled to room temperature and quenched with water (30 mL), and the solution was extracted three times with dichloromethane (3x 50 mL). The organic layer was washed with water (2x 20 mL) and saturated brine (50 mL), and the solution was dried by anhydrous magnesium sulfate. Following filtration, volatiles were removed *in-vacuo*, and the resulting residue was purified by column chromatography using hexane and dichloromethane (V_{hexane}: V_{CH2Cl2} =5:1) as eluent to afford compound **3a** as a green solid in 6% yield (31 mg): ^{1}H NMR (400 MHz, $CDCl_3$) δ 7.14 (d, *J* = 8.9 Hz, 4H), 7.08 (m, 18H), 7.02 (m, 12H), 6.92 (d, *J* = 7.6 Hz, 4H), 6.85 (d, *J* = 8.8 Hz, 8H), 6.27 (s, 2H), 3.84 (s, 6H) ppm. ^{13}C

NMR (100 MHz, $CDCl_3$) δ 157.4, 143.9, 143.8, 143.6, 141.3, 140.9, 140.8, 135.8, 133.2, 131.8, 131.7, 131.4, 131.4, 131.4, 131.1, 127.6, 127.2, 126.4, 114.2, 93.7, 55.5 ppm. HRMS (FTMS + p APCI): m/z+H^+ calcd for $C_{72}H_{54}N_2O_2$ 979.4258, found 979.4241.

3. RESULTS AND DISCUSSION

3.1 Synthetic procedures

Pyrrolo-[3,2-b]pyrroles represent a promising material for application in organic electronics with interesting optoelectronic properties and high synthetic versatility. However, the yields from different synthetic routes are still very low, which prevents their efficient use for industrial purposes.[43,44] With the addition of 10 mol% of *p*-toluene sulfonic acid as a catalyst to the reaction, this method was significantly improved in 2014, producing yields between 22 and 49%.[14] In this report, we present a method for the synthesis of tetraaryl-1,4-dihydropyrrolo-[3,2-b]pyrrole derivatives by multicomponent reactions employing *p*-toluenesulfonic acid as a catalyst.[14,43] The reactions were carried out under standard conditions (AcOH, 90 °C, 3 h) yielding compounds PP-Ar-OMe **1**, PP-Py **2** and PP-TPE **3** in 5%, 8% and 6% respectively. All compounds were fully characterized by $^1H/^{13}C$ NMR spectroscopy and high-resolution mass spectrometry (Figures S1-S9).

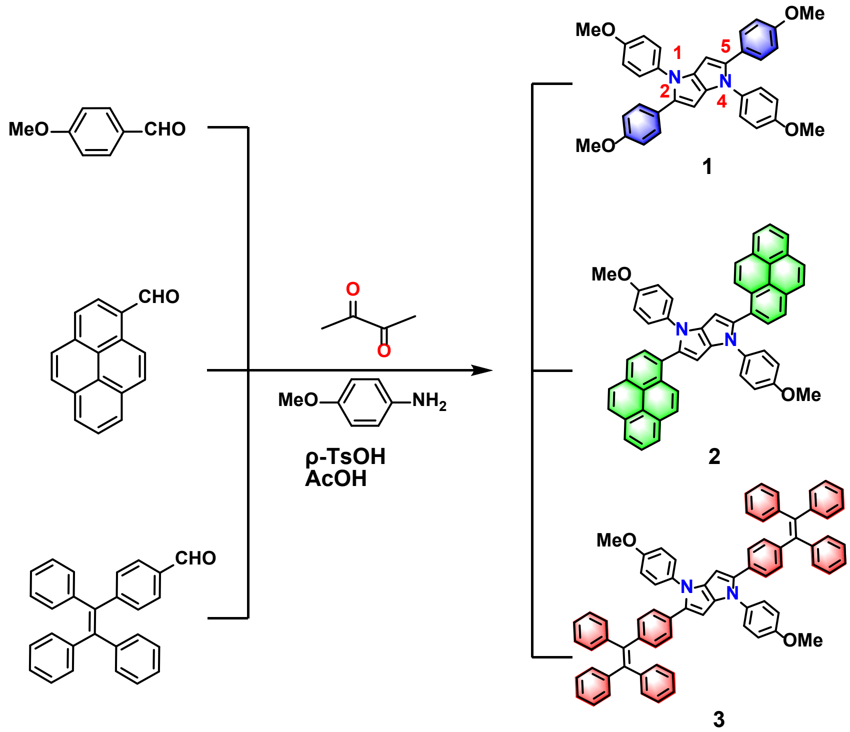

Scheme 1: Synthetic route to 1,4- dihydro-pyrrolo[3,2-b]pyrroles AIE derivatives.

3.2 Single-crystal X-ray diffraction analysis

To explore the influence of substituents on the molecular packing, a single crystal of compound **3** (CCDC 2290954) was successfully cultivated by the solvent diffusion method. The single crystal of **3** belongs to the monoclinic crystal system, with the space group C2/c. The related crystal parameters are summarized in Table S1. As shown in Figure 1, the phenyl ring is located at the 2,3-positions and 6- or 6,7-positions of the pyrrolo[3,2-b]pyrrole core, and they are arranged in a non-planar conformation. Due to the existence of steric hindrance, the average twist angle of the benzene ring at the 2,3-positions is significantly greater than the twist angle of the substituent at the 6-position or the 6,7-positions (Figure 1). On the other hand, the crystal **3** arranges in a shoulder-by-shoulder molecular packing, and there is no obvious π–π stacking between the molecules. The dominating intramolecular interactions originate from the C-H···π and C-H···O bond interactions with distances in the range 2.62–3.3 Å. Thus, a considerable number of weak interaction forces between molecules in crystal **3** effectively restrict the molecules rotation, suggesting possible emission behavior in the aggregated state.

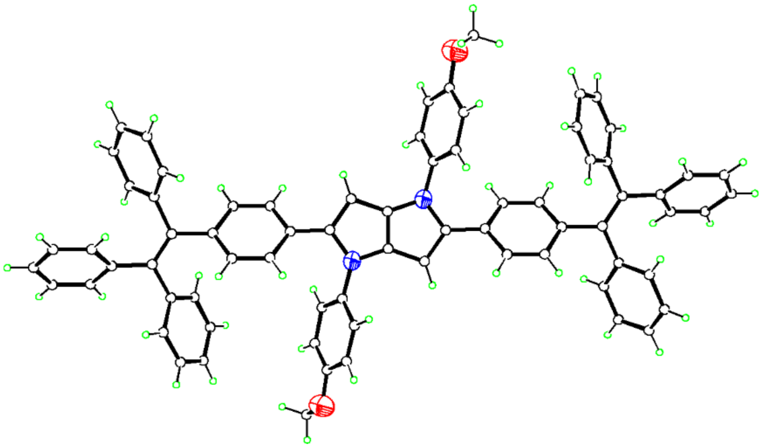

FIGURE 1. X-ray crystal structure of compound **3**; the ellipsoid probability is 30%.

3.3 Photophysical Properties

Preliminary photophysical characterization of the target compounds was carried out in light of the potential uses of tetraaryl-1,4-dihydropyrrolo-[3,2-b]pyrrole dyes in organic electronics. The UV-vis and emission spectra of **1**−**3** were measured in THF solution and the key parameters are summarized in Figure 2 and Tables 1. The organic dyes **1**−**3** exhibit broad absorption ranging from 300 to 380 nm, which were assigned to the π−π* transition of the aromatics. The long-wavelength absorption in the range 320-500 was ascribed to intramolecular charge transfer (ICT) through the whole push-pull conjugated system. The maximum absorption band is located at 345 nm with molar absorption coefficients (*ε*) of 4.1×10^4 M^{-1} cm^{-1} for **1**, 427 nm with *ε* 3.9×10^4 M^{-1} cm^{-1} for **2** and 1.0×10^5 M^{-1} cm^{-1} for **3,** respectively, which indicated that the expanded π−π* system results in the red-shifted maximum absorption peak.

In terms of the fluorescence, it was observed that dyes **2** and **3** bearing pyrene and tetraphenylethylene moieties as the conjugated bridge demonstrated significant, red-shifted emission in the green region with peak at 514 and 556 nm (Figure 2A), respectively. In contrast, dye **1** bearing *p*-methoxyphenyl moieties displayed a violet emission peak at 407 nm. Thus, the large red-shifted emissions for **2** and **3** can be associated with the extension of the π-conjugation length promoted by the presence of the pyrene and tetraphenylethylene groups.

Table 1. Electrochemical and absorption and emission data of the pyrene-based compounds **1−3**.

Compd.	ε ($\lambda_{\text{max abs}}$) (M^{-1} cm^{-1})$^{a)}$	λ_{maxPL} (nm) solns$^{a)}$/ films$^{b)}$	Φ_f solns$^{a)}$/ films$^{b)}$	τ (ns) solns$^{a)}$/ films$^{b)}$	k_r (10^8 s^{-1})^c solns$^{a)}$/ films$^{b)}$	k_{nr} (10^8 s^{-1})^d solns$^{a)}$/ films$^{b)}$
1	345 (4.1×10^4)	407/430	0.83/0.03	1.30/0.67	6.38/44.8	1.31/14.5
2	427 (3.9×10^4)	514/504	0.75/0.51	2.34/1.00	3.21/5.10	1.07/4.90
3	401 (1.0×10^5)	556/507	0.02/0.78	0.72/1.86	0.28/4.19	13.6/1.18

[a] Maximum absorption wavelength measured in THF solution at room temperature. [b)] Measured in the solid state. [c)] k_r = radiative decay rate (Φ/τ). d) k_{nr} = nonradiative decay rate (1/τ- k_r)

The restriction of intramolecular rotation (RIM) has been proposed as an explanation for the enhancement of luminescence during the aggregation process.[45] According to the RIM mechanism, the peripheral phenyl rings can rotate freely and the excited energy is released by a non-radiation pathway, while on restricting the molecular motion, the non-radiation pathway is blocked in the aggregated state, resulting in a radiative transition process, accompany with an enhanced emission.

Dong and Tang *et al*. simultaneously reported that if electron-withdrawing groups are placed at the 1- and 4- positions of the tetraarylpyrrolo[3,2-b]pyrrole (TAPPs) TAPP core, then fantastic AIE behavior is achieved.[46-49] Inspired by the molecular structures of compounds **1−3**, the peripheral phenyl (pyrene) rings are regarded as rotators using the pyrrolo[3,2-b]pyrroles as the core, and thus they have potential to display AIE characteristics.[30] Therefore, to examine the AIE characteristics of the 1,4-dihydro-pyrrolo[3,2-b]pyrrole derivatives **1−3**, the fluorescence spectra were measured in THF containing different water fractions (f_w) and the results are presented in Figures 2C and S13. Compounds **1−3** show maximum emission peaks at $\lambda_{max\ em}$ = 407, 514 and 556 nm in THF solution, with fluorescence quantum yields of 0.83 for **1**, 0.75 for **2** and 0.02 for **3** respectively. As the f_w increased from 0 to 90%, the emission intensity of compound **3** was enhanced *ca*. 6-fold, compared with its fluorescence intensity in pure THF solution (Figure 2D). The quantum yield of **3** in the film was enhanced 39-fold and up to 0.78 compared to its THF solution. In the case of the pyrene containing dihydropyrrolo-[3,2-b] pyrrole **2**, as the f_w increased from 0 to 30%, the emission intensity of compound **2** was enhanced *ca*. 4-fold, compared with its fluorescence intensity in pure THF solution (Figure S13), However, when the f_w increased to 99%, the emission intensity was decreased with a red-shifted emission at $\lambda_{max\ em}$ = 527 nm, which originated from the strong intermolecular interactions in the aggregated state. The maximum emission peak of compounds **1-3** are at 430, 504 and 507 nm with fluorescence quantum yields of 0.03. 0.51 and 0.78 (Figure 2B), respectively. On the other hand, the fluorescence lifetime for these compounds **3** were also measured in the range of 0.72~2.34 nm, and the calculated radiative decay rate (k_r) and non- radiative decay rate (k_{nr}) are summarized in Table 1. The k_r and k_{nr} of both compounds **1** and **2** increased, while the calculated k_r of **3** increased from 0.28×10^8 s^{-1} to 4.19×10^8 s^{-1}, while the k_{nr} decreased from 13.6×10^8 s^{-1} to 1.18×10^8 s^{-1}. Thus, according to the results, compound **3** containing TPE units is AIE-active, whilst compounds **1** and **2** are non-AIE active molecules. In addition, the blue shifted emission for compound **2** is ascribing to the H-aggregation between the pyrene core in the thin film.[50]

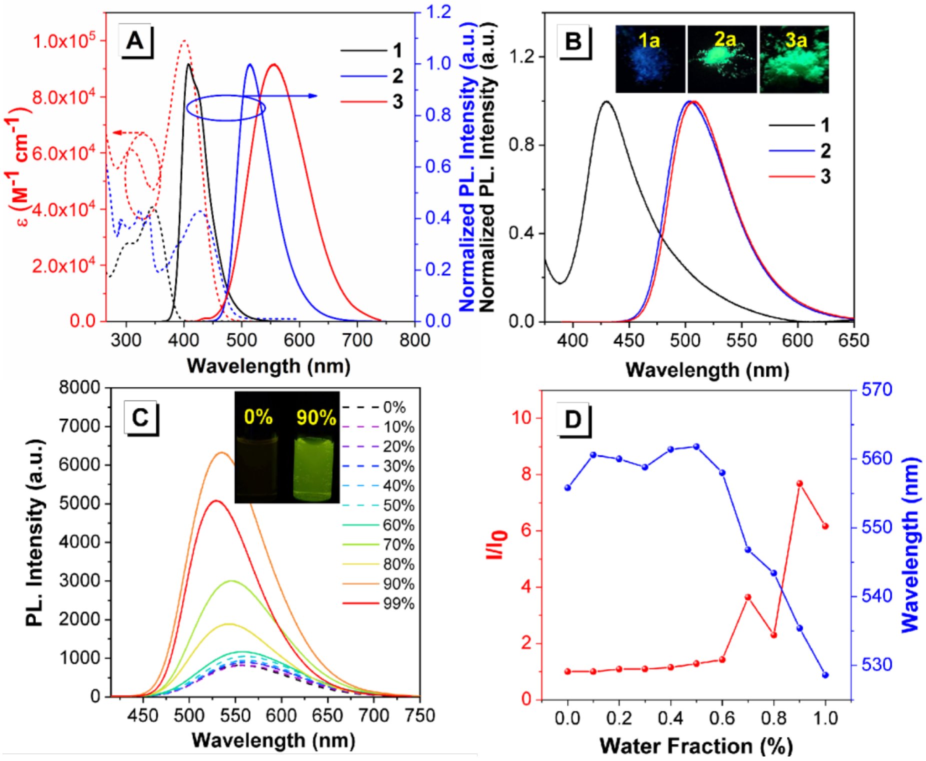

FIGURE 2. (A) UV-vis and emission spectra of compounds **1**−**3** in THF (~10 μM); (B) emission spectra of **1**−**3** in the solid state, insert: the photographs of compounds **1**−**3** under UV irradiation (λ_{ex} = 365 nm); (C) emission spectra of compound **3** in mixed THF/H_2O with various water fractions; (D) Plot of relative PL intensity (I/I_0) *versus* the composition of the THF/water mixture of **3**.

The concentration-dependent PL spectra of the pyrrolo[3,2-b]pyrrole derivatives **1-3** were studied in THF solution ([M] = 10^{-7}–10^{-3} M) (Figure S14). As the concentration was increased from 10^{-7} to 10^{-3} M, the compounds **1** and **2** slightly changed, and this may be due to the molecular conformation which can regulate the intramolecular interactions, and efficiently suppress the π-π stacking. For compound **3**, the maximum emission peak was red-shifted to 575 nm as the concentration increased to 10^{-3} M. The concentration-dependent bathochromic phenomenon may be due to the formation of molecular aggregated species (dimers, trimers, etc.), which leads to a multiple photoluminescence phenomenon. Furthermore, solvent effects for the pyrrolo[3,2-b]pyrrole derivatives **1**−**3** were measured in cyclohexane, tetrahydrofuran, 1,4-

dioxane, dimethylformamide (DMF), acetonitrile (ACN) and dimethylsulfoxide (DMSO) (Figures S15-S17, Table S2). The solvent polarity showed only a limited effect on the absorption and emission behavior. Although the compounds **2** and **3** exhibit a slightly blue-shifted absorption peak (5 nm for **2**, 4 nm for **3**), the emission was red-shifted more than 50 nm on increasing the solvent polarity.

3.4 DFT theoretical calculations

In order to further explore the influence of the π-conjugation length on the electronic structure and properties of the target molecules, density functional theory (DFT) calculations were performed using Gaussian 09W at the basis set level of B3LYP/6-311G(d,p).[51] The energies of the highest occupied molecular orbital (HOMO) and the lowest unoccupied molecular orbital (LUMO) levels and the ground state are shown in Figure 3. The HOMO energy levels of molecules **1-3** are mainly concentrated on the pyrrolo[3,2-b]pyrroles skeleton and the aromatic groups at the 2,5-positions of the pyrrolo[3,2-b]pyrrole cores. Meanwhile, due to the electronic effect of the substituents at the 1,4-positions, the electronic distribution in the LUMO energy level is different. For example, in the case of compound **1**, the LUMO energy level is distributed over the whole molecular structure, while the LUMO energy of compounds **2** and **3** is mainly concentrated on the pyrene moieties and TPE units, respectively. In addition, the energy gaps of compounds **1**–**3** are 3.87, 2.93 and 3.13 eV, respectively.

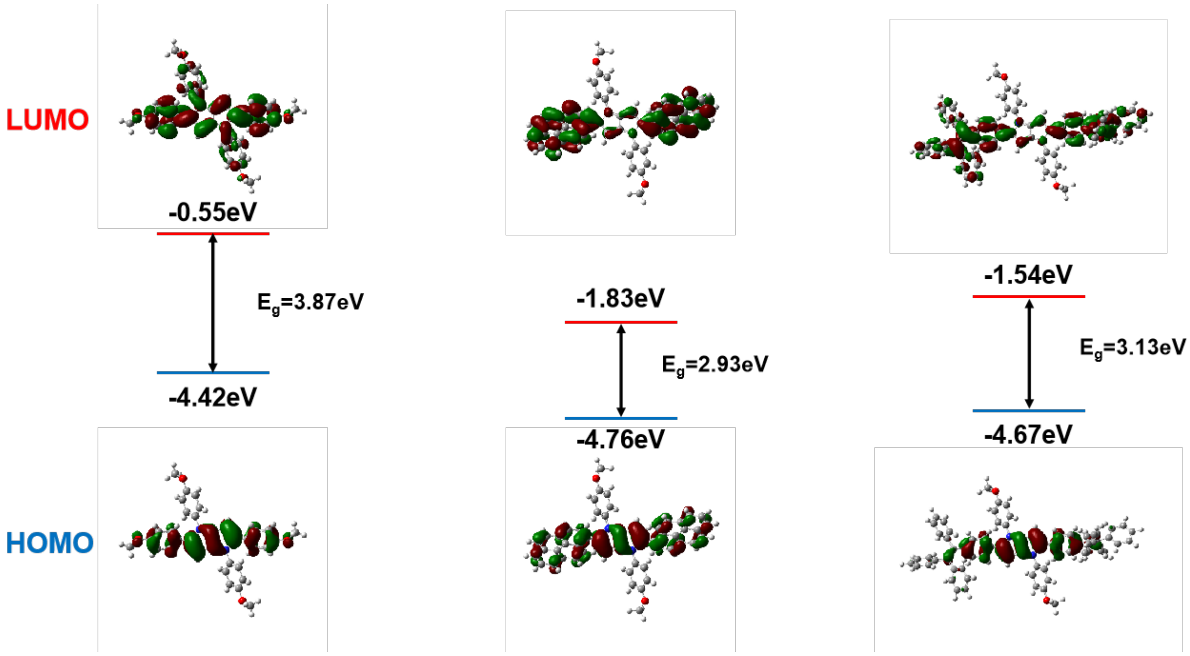

FIGURE 3. Molecular orbital energy distribution of compounds **1**–**3** calculated by B3LYP/6-31 G (d.p).

3.5 Dichloromethane and chloroform detection

Interestingly, compound **1** exhibits high sensitivity and selectivity toward dichloromethane (CH_2Cl_2) and chloroform ($CHCl_3$) solvent molecules. For example, the maximum absorption band of compound **1** in CH_2Cl_2 is at 343nm, and the absorption intensity decreased with two new absorption bands at 456 nm 624 nm appearing after UV irradiation. The solution color changed from colorless to light-yellow, indicating that a new species was produced (Figure 4A). Upon excitation, compound **1** emitted a deep blue fluorescence with a maximum emission peak at 409 nm in CH_2Cl_2. Under UV irradiation, two new emission peaks at 501 nm and 610 nm appeared (λ_{ex} = 340 nm), and the new emission intensity (λ_{em} =501 nm) was enhanced as the irradiation time was extended from 0 to 60s; the emission color was tuned from blue to pink (Figure 4B). Moreover, using λ_{ex} = 450 nm as excitation source, compound **1** showed a dual emission with two emission peaks at 501 and 610 nm, respectively, which could further be enhanced after irradiation over 60 s (Figure S18). Although we could not identify the detailed molecular structure by ^{1}H NMR spectroscopy, a molecular peak at m/z$^+$ at 579.21 was observed, which is assigned to the **1@CH$_2$Cl** species, indicating that compound **1** can react with CH_2Cl_2 to achieve a new species **1@CH$_2$Cl** under UV irradiation (Figure S10). Similarly, compound **1** in $CHCl_3$ also showed similar phenomenon under UV irradiation, with the maximum absorption band of compound **1** in $CHCl_3$ at 340 nm. After irradiation for 5s, two new broad absorption bands with λ_{max} abs at 425 nm and 725 nm appeared. Subsequently, both absorption bands decreased and were blue-shifted to 411 nm 627 nm upon irradiation for 10s, and the absorption intensity remained stable after irradiation for 60s. Moreover, the solution color changed from colorless to light-green (Figure 4C). Upon excitation, compound **1** emitted a deep blue fluorescence with a maximum emission peak at 413 nm in $CHCl_3$. Under UV irradiation, a new emission peak at 510 nm appeared (λ_{ex} = 340 nm), and the emission intensity enhanced as the irradiation time extending from 0 to 60s with the emission color tuned from deep blue to green (Figure 4D). The irradiated sample was characterized by mass spectrometry with m/z$^+$ of 613.17 (Figure S11), indicated that a new species **1@CHCl$_2$** was achieved. On the other hand, both species **1@CH$_2$Cl** and **1@CHCl$_2$** cannot be recovered after removing the UV light. In addition, compound **1** did not show this phenomenon in other solvents, such as hexane, THF, 1，4-dioxane, THF, DMF, ACN solvent (Figures S19-23). Thus, the compound **1** exhibits a high sensitivity toward dichloromethane and chloroform detection.

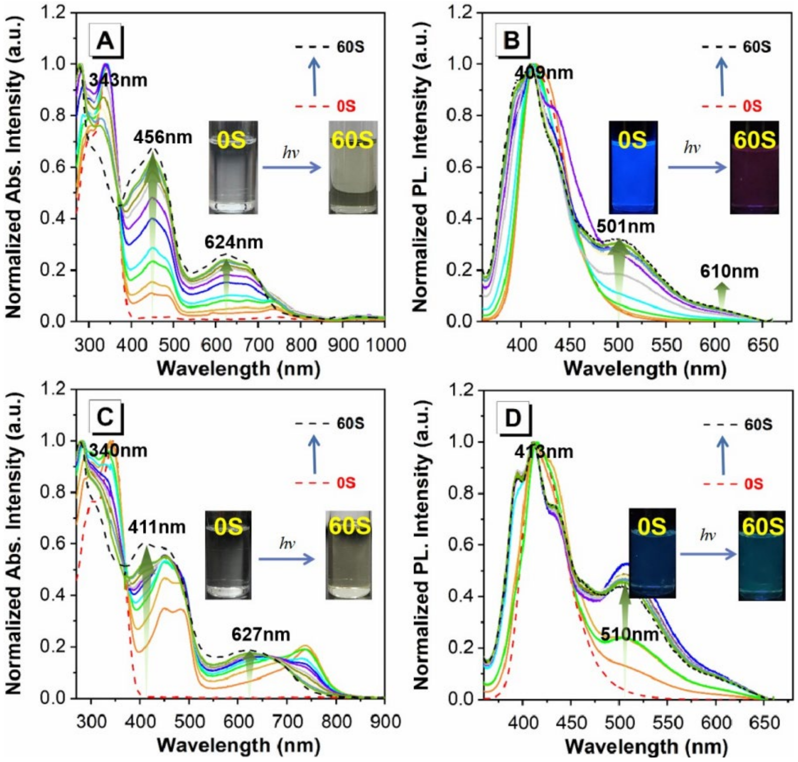

FIGURE 4. UV-vis and emission spectra of compound **1** (A) and (B) in CH_2Cl_2, (C) and (D) in $CHCl_3$ under UV irradiation.

4. CONCLUSION

In summary, using a pyrrolo[3,2-b]pyrrole as the building block, three blue or green emitters were synthesized by a multicomponent reaction in relatively low yield. Although four rotators were introduced into the pyrrolo[3,2-b]pyrrole core, only compound **3** containing tetraphenylethylene moieties exhibits a typical AIE feature. DFT calculations were performed in order to investigate the charge distribution in the molecule and the impact of the energy levels on the luminescence's color shift. Moreover, compound **1** exhibits high sensitivity and selectivity toward dichloromethane (CH_2Cl_2) and chloroform ($CHCl_3$) under UV irradiation with a visible emission color change. Both UV-vis and absorption and HRMS spectra indicated tht compound

1 could react with CH_2Cl_2 and $CHCl_3$ to produce a new species. This article presents a new method to detect the solvents dichloromethane (CH_2Cl_2) and chloroform ($CHCl_3$).

DECLARATION OF COMPETING INTEREST

The authors declare that they have no conflict of interest.

DATA AVAILABILITY STATEMENT

Data available on request from the authors

ACKNOWLEDGEMENTS

This work was supported by the National Natural Science Foundation of China (21975054), Guangdong Provincial Key Laboratory of Information Photonics Technology (2020B121201011), Natural Science Foundation of Guangdong Province of China (2019A1515010925), the Open Fund of Guangdong Provincial Key Laboratory of Luminescence from Molecular Aggregates, Guangzhou 510640, China (South China University of Technology) (2019B030301003) and Science and Technology Planning Project of Hunan Province (2018TP1017), M. M. Islam thanks to MOST, P. R. China for Talented Young Scientist Program (TYSP) Fellowship. CR thanks the University of Hull for support.

ORCID

Md. Monarul Islam, https://orcid.org/0000-0002-4117-4862

Xing Feng, https://orcid.org/ 0000-0002-4273-979X

REFERENCES

[1] M. M. Islam, Z. Hu, Q. Wang, C. Redshaw, X. Feng, *Mater. Chem. Front.* **2019**, *3*, 762.

[2] X. Feng, J. Zhang, Z. Hu, Q. Wang, M. M. Islam, J.-S. Ni, M. R. J. Elsegood, J. W. Y. Lam, E. Zhou, B. Z. Tang, *J. Mater. Chem. C*, **2019**, *7*, 6932.

[3] M. Mohan, J. James, M.N. Satyanarayan, D. R. Trivedi, *Luminescence*. **2019**, 33, 715.

[4] A. Karuppusamy, P. Kannan, K. Rajakumar, D. Zherebtsov, *Luminescence*. **2021**, *36*, 1048.

[5] S. Zhang, T. Wang, X. Wang, W. Liao, X. Wang, Y. Yuan, G. Chen, X. Jia, *Luminescence*. **2022,** *37*, 2139.

[6] C. Micheletti, Q. Wang, F. Ventura, M. Turelli, I. Ciofini, C. Adamo, A. Pucci, *Aggregate*. **2022**, *3*, e188.

[7] J. Zhang, Q. Wei, W. Li, H. Chen, X. Zhu, Y. Bai, N. Fei, L. Cao, Z. Zhao, A. Qin, B. Z. Tang, Z. Ge, *Aggregate.* **2023**, e410.

[8] M. Zhang, W. Zhao, *Aggregate*.**2021**, *2*, e60

[9] A. Janiga, D. T. Gryko, *Chem.-Asian J.* **2014**, *9*, 3036; (b) M. Krzeszewski, D. Gryko, D. T. Gryko, *Acc. Chem. Res*. **2017**, *50*, 2334.

[10] M. Tasior, B. Koszarna, D. C. Young, B. Bernard, D. Jacquemin, D. Gryko, D. T. Gryko, *Org. Chem. Front.* **2019**, *6*, 2939.

[11] A. Krutosíkova, T. Gracza, Topics in heterocyclic chemistry. **2008**.

[12] A. K. Biswas, A. Das, B. Ganguly, *New J. Chem*. **2016**, *40*, 9304.

[13] A. Capan, H. Veisi, A. Goren, T. Ozturk. *Macromolecules* **2012**, *45*, 8228.

[14] M. Krzeszewski, B. Thorsted, J. Brewer, D. T. Gryko, *J. Org. Chem.* **2014**, *79*, 3119.

[15] S. Shinamura, I. Osaka, E. Miyazaki, K. Takimiya, *Heterocycles*. **2011**, *83*, 1187.

[16] 18M. Banasiewicz, R. Stęzycki, D. G. Kumar, M. Krzeszewski, M. Tasior, B. Koszarna, A.˙ Janiga, O. Vakuliuk, B. Sadowski, D. T. Gryko, D. Jacquemin, *Eur. J. Org. Chem.* **2019**, 5247.

[17] J. Luo, Z. Xie, J. W. Y. Lam, L. Cheng, H. Chen, C. Qiu, H. S. Kwok, X. Zhan, Y. Liu, D. Zhu, B. Z. Tang, *Chem. Commun*. **2001**, 1740.

[18] B.-K. An, S.-K Kwon, S.-D. Jung, S. Y. Park, *J. Am. Chem. Soc.* **2002**, *124*, 14410.

[19] Z. Hu, Y. Li, M. Kang, M. M. Islam, M. Chen, J. Zhang, Y. Xiao, X. Feng, C. Redshaw, M. Zhang, Q. Chen, S. Xie, J. W. Y. Lam, B. Z. Tang, *EcoMat*. **2020**, *2*, e12024

[20] Z. Hu, H. Zhang, Y. Chen, Q. Wang, M. R. J. Elsegood, S. J. Teat, X. Feng, M. M. Islam, F. Wu, B. Z. Tang, *Dyes Pigm.* **2020**, *175*, 108175.

[21] G. Lin, L. Chen, H. Peng, S. Chen, Z. Zhuang, Y. Li, B. Wang, Z. Zhao, B. Z. Tang, *J. Mater. Chem. C* **2017**, 5, 4867

[22] J. Guo, S. Hu, W. Luo, R. Hu, A. Qin, Z. Zhao, B. Z. Tang, *Chem. Commun.* **2017**, *53*, 1463.

[23] X. Li, M. Jiang, J. W. Y. Lam, B. Z. Tang, J. Y. Qu, *J. Am. Chem. Soc.* **2017**, *139*, 17022.

[24] S. Zhang, D. Li, X. Wang, J. Fan, T. Wang, S. Yu, W. Liao, X. Jia, Y. Yuan, *Luminescence*. **2021**, *36*, 958;

[25] M. Guo, W. Li, Y. Sun, H. Xu, Y. Fan, L. Ma, K. Huang, Z. Yao, *Luminescence*. **2019**, *34*, 558.

[26] A. I. Ivanov, B. Dereka, E. J. Vauthey, *Chem. Phys.* **2017**, *146*, 164306.

[27] H. Liu, J. Ye, Y. Zhou, L. Fu, Q. Lu, C. Zhang, *Tetrahedron Lett.* **2017**, *58*, 4841.

[28] B. Dereka, E. J. Vauthey, *Chem. Sci.* **2017**, *8*, 5057.

[29] J.-Y. Wu, C.-H. Yu, J.-J. Wen, C.-L. Chang, M. Leung, *Anal. Chem.* **2016**, *88*, 1195.

[30] K. Li, Y. Liu, Y. Li, Q. Feng, H. Hou and B. Z. Tang, *Chem. Sci.*, **2017**, *8*, 7258-7267.

[31] J. Wang, Z. Chai, S. Liu, M. Fang, K. Chang, M. Han, L. Hong, H. Han, Q. Li, Z. Li, *Recombination. Chem. Eur. J.* **2018**, *24*, 18032.

[32] R. Domínguez, N. F. Montcada, P. de la Cruz, E. Palomares, F. Langa, *ChemPlusChem* **2017**, *82*, 1096.

[33] Y. Zhou, M. Zhang, J. Ye, H. Liu, K. Wang, Y. Yuan, Y.- Q. Du, C. Zhang, C.-J. Zheng, X.-H. Zhang, *Org. Electron*. **2019**, 65, 110.

[34] R. K. C. Balasubramanyam, R. Kumar, S. J. Ippolito, S. K. Bhargava, S. R. Periasamy, R. Narayan, P. Basak, *J. Phys. Chem. C* **2016**, *120*, 11313.

[35] Y. Ma, Y. Zhang, L. Kong, J. Yang, *Molecules* **2018**, *23*, 3255.

[36] C. S. Hawes, G. M. Ó Maille, K. Byrne, W. Schmitt, T.´ Gunnlaugsson, *Dalton Trans*. **2018**, *47*, 10080.

[37] L. M. Martins, S. de F. Vieira, G. B. Baldacim, B. A. Bregadiolli, J. C. Caraschi, A. B.-Neto, L. C. da S.-Filho, *Dyes Pigm.* **2018**, *148*, 81.

[38] J. Wang, Z. Chai, S. Liu, M. Fang, K. Chang, M. Han, L. Hong, H. Han, Q. Li, Z. Li, *Chem. Eur. J.* **2018**, *5*, 18032.

[39] W. Liu, G. Hong, D. Dai, L. Li, M. Dolg. *Theor. Chem. Acc*. **1997**, 96, 75 - 83.

[40] Y. Zhang, B. Suo, Z. Wang, N. Zhang, Z. Li, Y. Lei, W. Zou, J. Gao, D. Peng, Z. Pu, Y. Xiao, Q. Sun, F. Wang, Y. Ma, X. Wang, Ya Guo, and Wenjian Liu. *J. Chem. Phys*., **2020**, 152, 064113.

[41] S. W. Liu, F. Wang, L. Li. *J. Theor. Comput. Chem*. **2003**, 02, 257 – 272.

[42] W. Liu, F. Wang, L. Li. Relativistic Density Functional Theory: The BDF Program Package, chapter 9, pages 257 – 282. Volume 5. World Scientific Publishing, **2004**.

[43] M. Tasior, O. Vakuliuk, D. Koga, B. Koszarna, K. Górski, M. Grzybowski, Ł. Kielesinski, M. Krzeszewski, D. T. Gryko, *J. Org. Chem.* **2020**, *85*, 13529.

[44] T. Kumagai, S. Tanaka, T. Mukai, *Tet. Lett.* **1984**, 25, 5669.

[45] N. L. C. Leung, N. Xie, W. Yuan, Y. Liu, Q. Wu, Q. Peng, Q. Miao, J. W. Y. Lam, B. Z. Tang, *Chem. Eur. J.* **2014**, *20*, 15349.

[46] R. Domínguez, N. F. Montcada, P. de la Cruz, E. Palomares, F. Langa, *ChemPlusChem* **2017**, *82*, 1096.

[47] S. Mishra, M. Krzeszewski, C. A. Pignedoli, P. Ruffieux, R. Fasel, G. D. Gryko, *Nat. Commun.* **2018**, *9*, 1714.

[48] K. Li, Y. Liu, Y. Li, Q. Feng, H. Hou, B. Z. Tang, *Chem. Sci.* **2017**, *8*, 7258.

[49] Y. Ji, Z. Peng, B. Tong, J. Shi, J. Zhi, Y. Dong, Y. *Dyes Pigm.* **2017**, *139*, 664.

[50] X. Feng, X. Wang, C. Redshaw, B. Z. Tang, *Chem. Soc. Rev.* **2023**, *52*, 6715-6753

[51] M. J. T. Frisch, Gaussian 09, revision A. 02, Gaussian, Inc., Pittsburgh, PA, **2009.**